Supporting Information

Molybdenum sulfo-oxide/cobalt oxysulfide Z-scheme heterojunction catalyst for efficient photocatalytic hydrogen production and pollutants reduction

Qinhan Wu[1], Adugna Boke Abdeta[1], Dong-Hau Kuo[2,*], Hanya Zhang[1], Qingxin Lu[1], Jubin Zhang[1,*], Osman Ahmed Zelekew[3], Mengistu Tadesse Mosisa[1], Jinguo Lin[1,*], Xiaoyun Chen[1,*]

[1]College of Materials Engineering, Fujian Agriculture and Forestry University, Fuzhou 350002, China

[2]Department of Materials Science and Engineering, National Taiwan University of Science and Technology, Taipei 10607, Taiwan

[3]Department of Materials Science and Engineering, Adama Science and Technology University, Adama, Ethiopia

*Corresponding author

E-mail address: dhkuo@mail.ntust.edu.tw (D.-H. Kuo)

E-mail address: zhangjubinfzu@163.com (J. B. Zhang)

E-mail address: fjlinjg@126.com (J. G. Lin)

E-mail address: fjchenxy@126.com (X. Y. Chen)

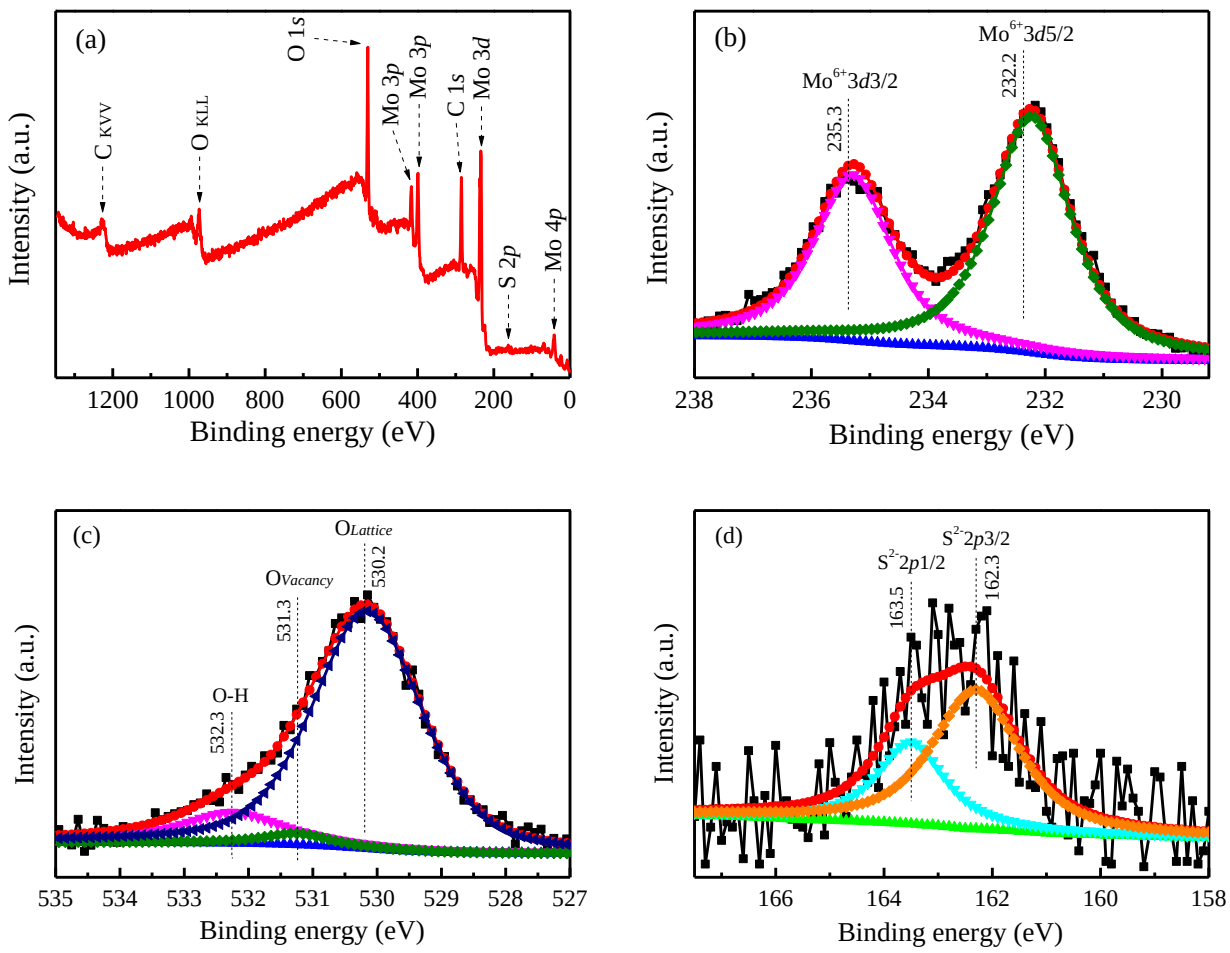

Fig. S1 (a) Survey spectra and high resolution XPS spectra of (b) Mo3*d*, (c) O1*s*, and (d) S2*p* of Mo(S,O).

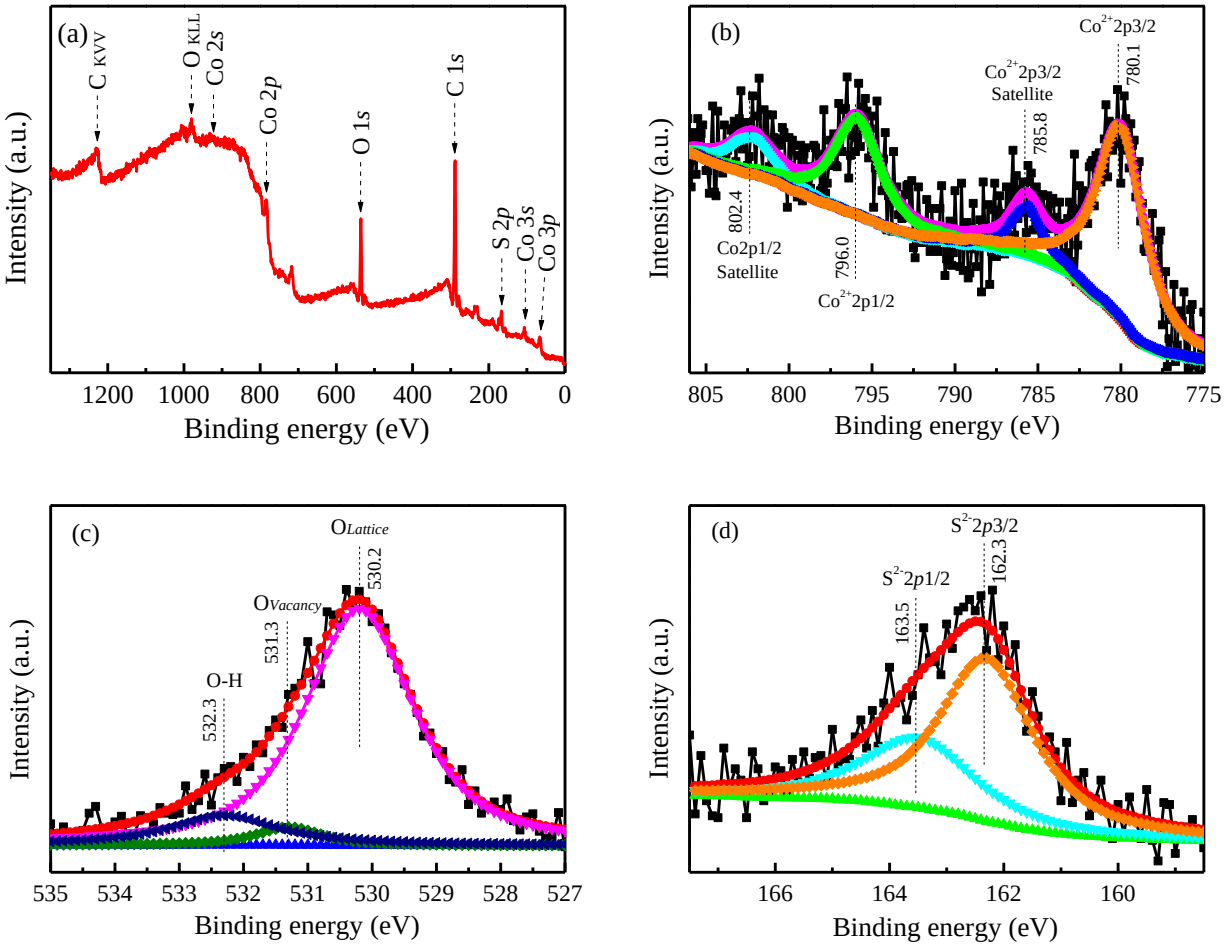

Fig. S2 (a) Survey spectra and high resolution XPS spectra of (b) Co2*p*, (c) O1*s*, and (d) S2*p* of Co(O,S).

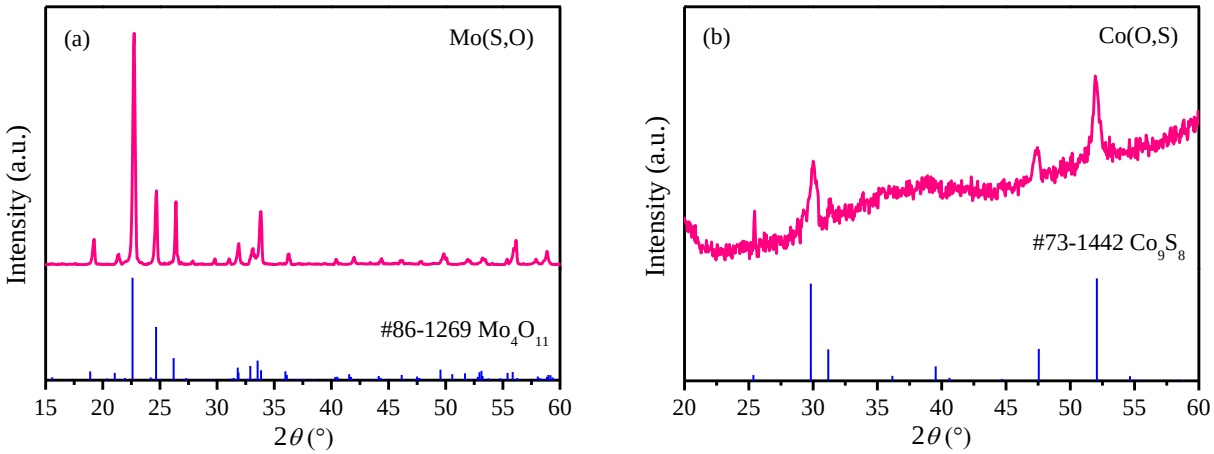

Fig. S3 (a) XRD diffraction pattern of Mo(S,O) and the Mo_4O_{11} standard of PDF 86-1269. (b) XRD diffraction pattern of Co(O,S) and the Co_9S_8 standard of PDF 73-1442.

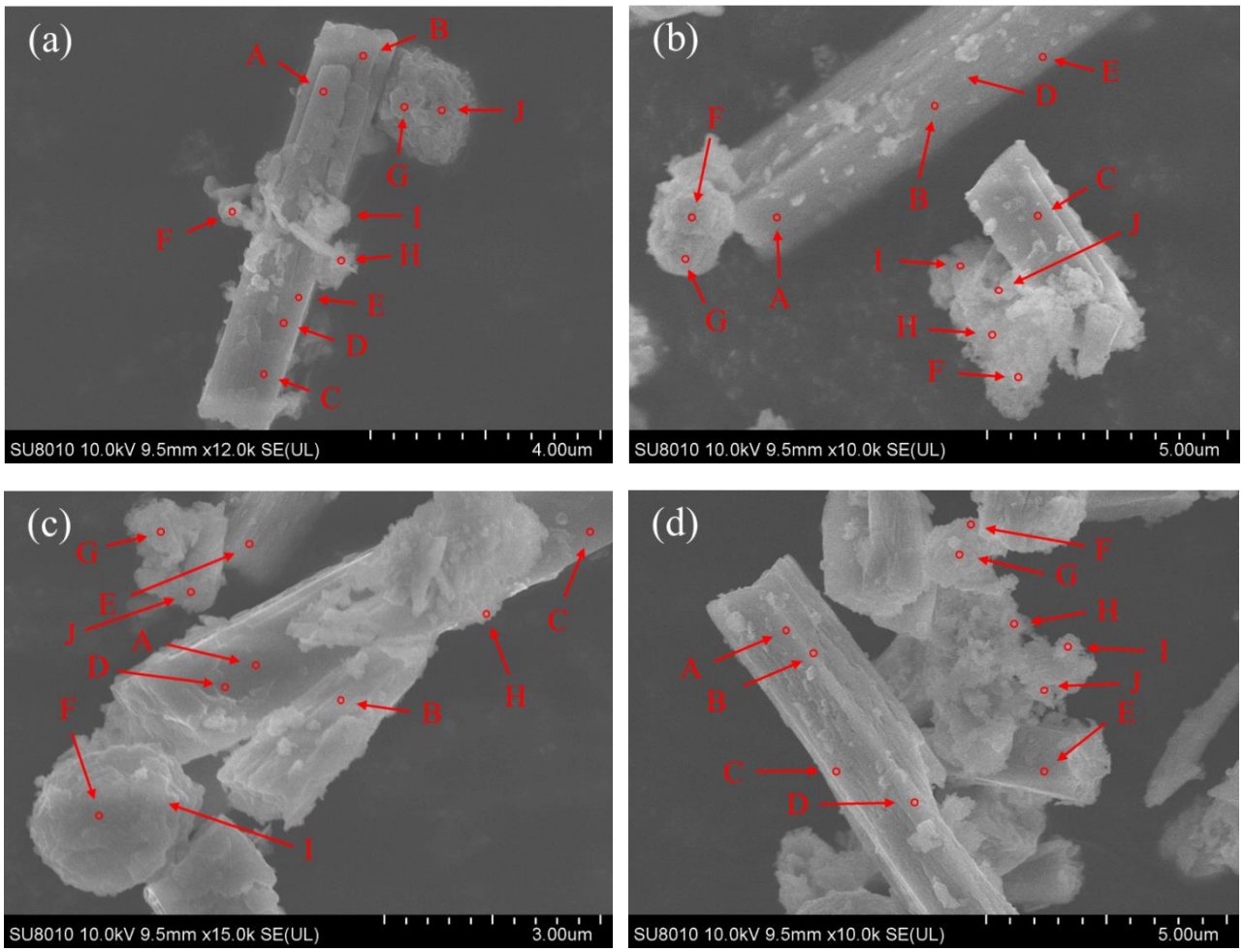

Fig. S4 SEM images of MoCoOS-1, MoCoOS-2, MoCoOS-3, and MoCoOS-4.

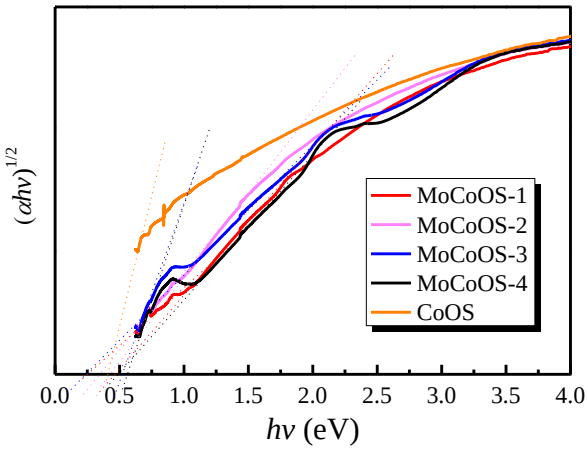

Fig. S5 The $(\alpha h\nu)^{1/2}$-$h\nu$ plots from the ultraviolet absorption spectra.

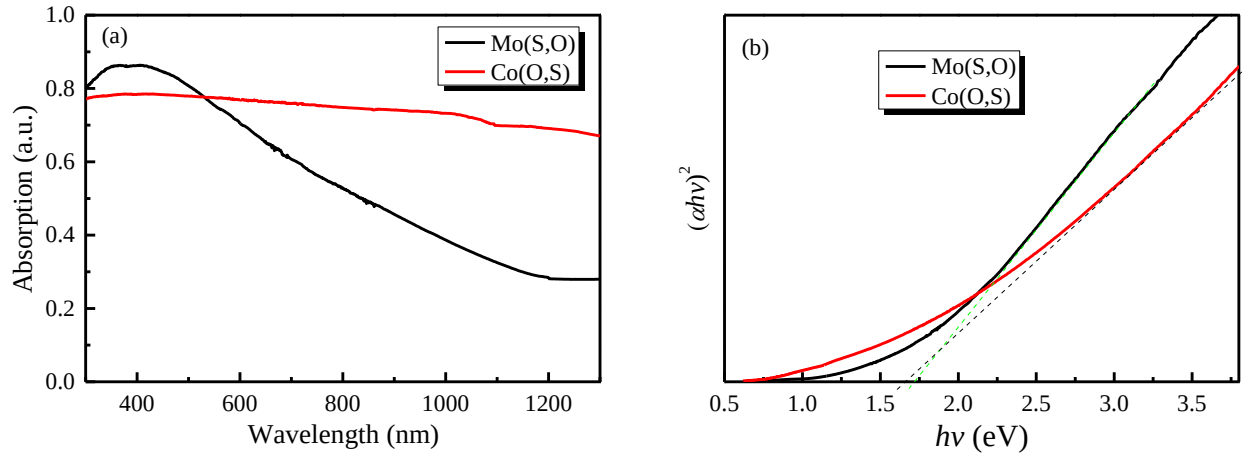

Fig. S6 (a) UV-Vis absorption spectra and (b) the $(\alpha h\nu)^2$-$h\nu$ plots of Mo(S,O) and Co(O,S) from the UV-Vis absorption spectra.

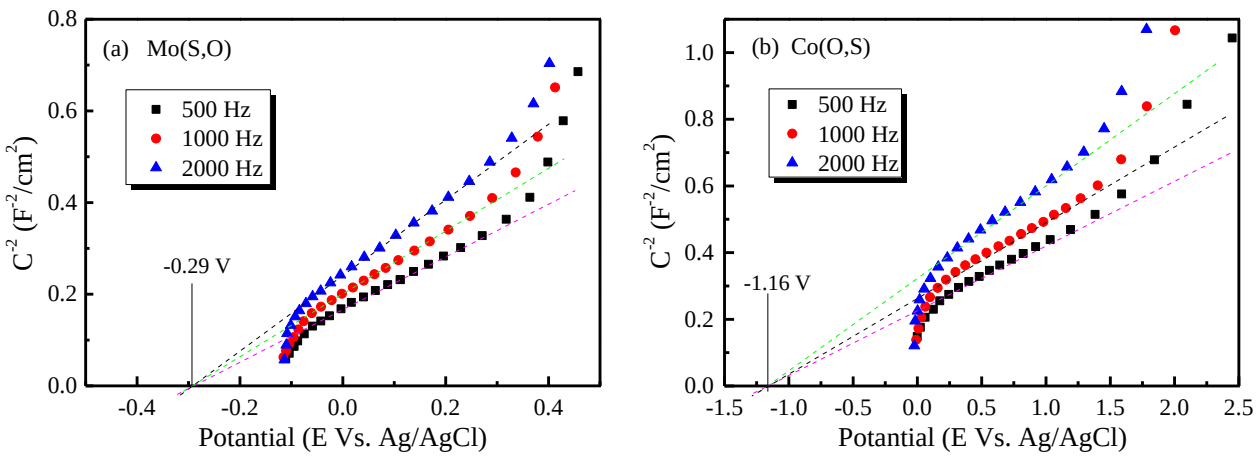

Fig. S7 Mott-Schottky curves of (a) Mo(S,O) and (b) Co(O,S).

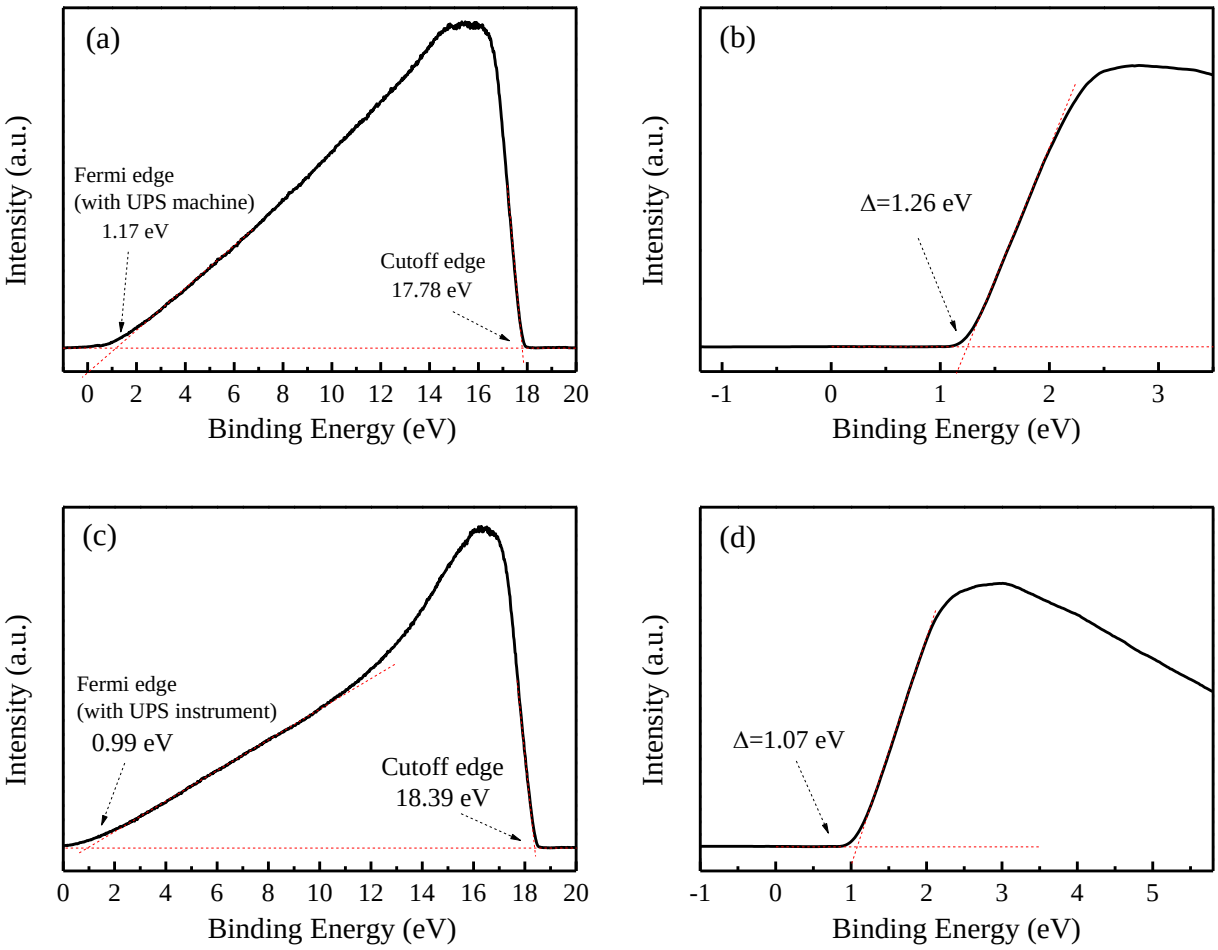

Fig. S8 (a) The UPS spectrum and (b) XPS-VB spectrum of Mo(S,O). (c) The UPS spectrum and (d) XPS-VB spectrum of Co(O,S).

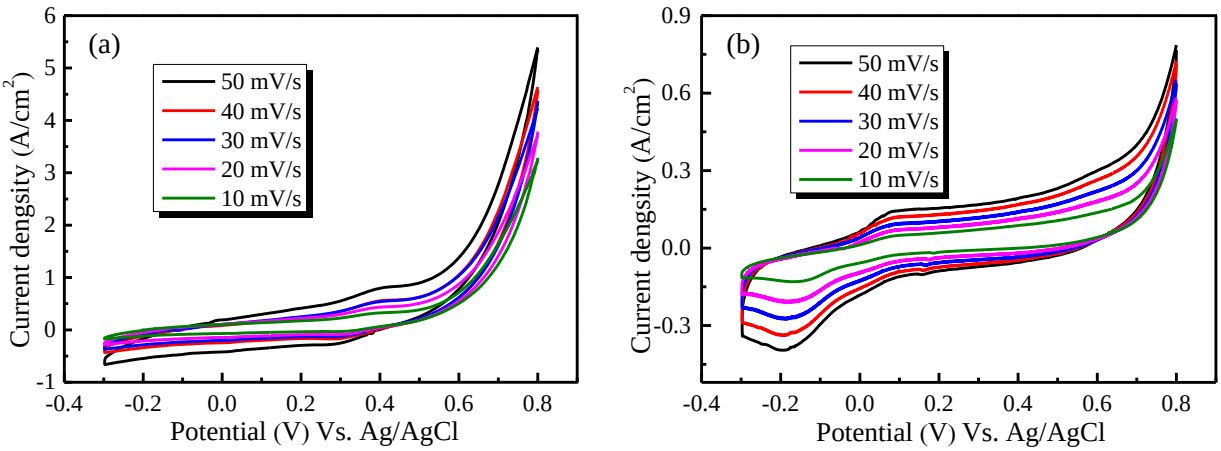

Fig. S9 The current density plots of (a) Mo(S,O) and (b) Co(O,S) catalysts under different scan rates.

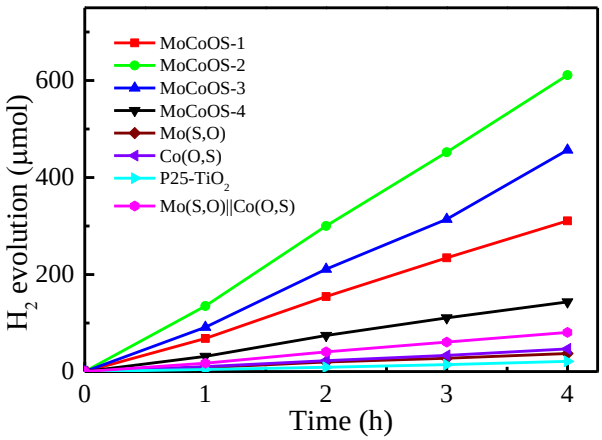

Fig. S10 Hydrogen production of MoCoOS, Mo(S,O), Co(O,S), Mo(S,O)||Co(O,S) and P25-TiO_2 catalysts.

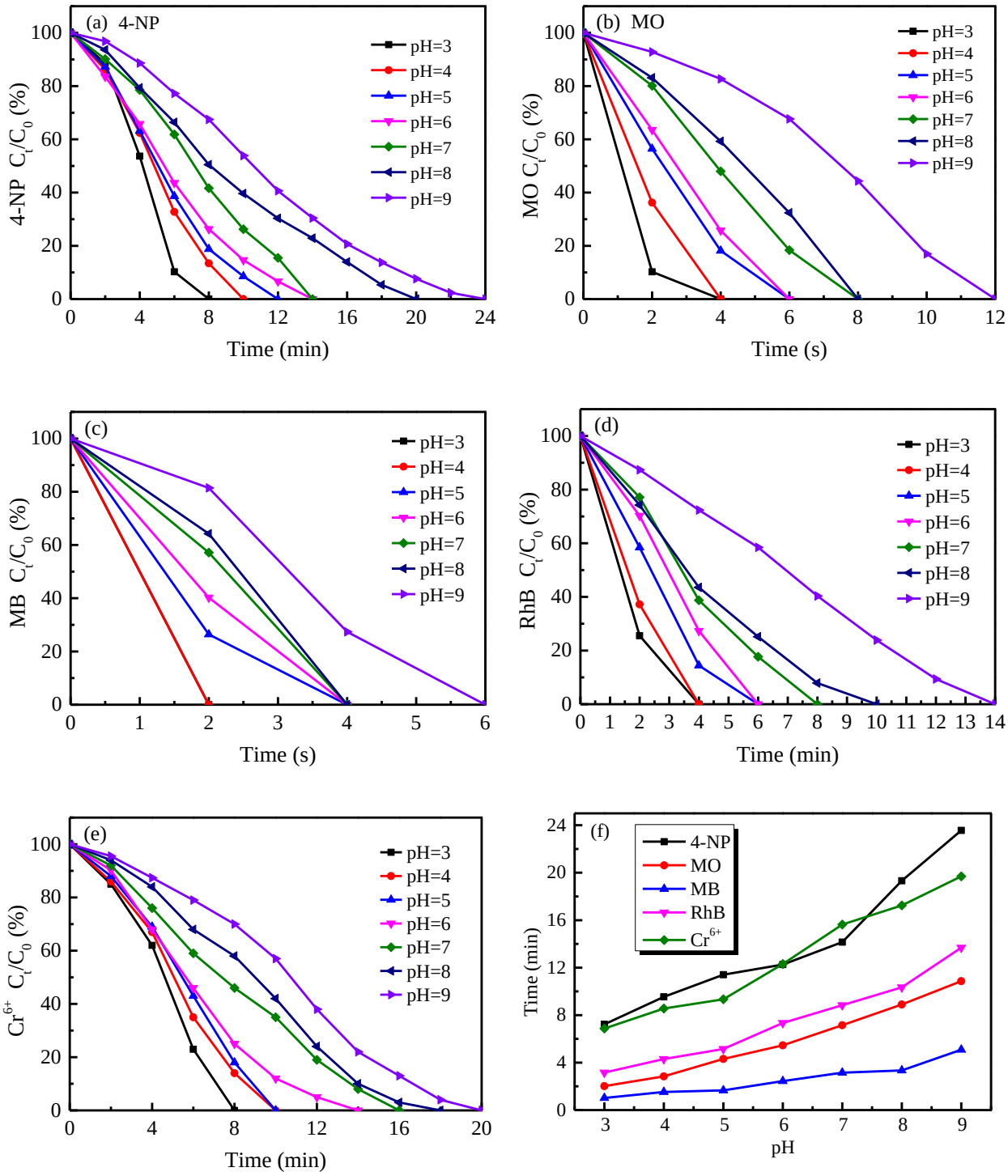

Fig. S11 (a)-(e) Reduction of 4-NP, MO, MB, RhB, and Cr^{6+} by MoCoOS-2 under different pH conditions. (f) The time to complete reduction of 4-NP, MO, MB, RhB, and Cr^{6+} by MoCoOS-2 under different pH conditions.

Table S1 XPS composition, crystal size and S_{BET} analyses of Mo(S,O), Co(O,S), and MoCoOS catalysts

Catalyst	Elements percentage (%)				O percentage (%)			Crystal size * (nm)		S_{BET} (m^2/g)	n[Co(O,S)]/ n[Co(O,S)]+n[Mo(S,O)]
	Mo	Co	O	S	$O_{Lattice}$	$O_{Vacancy}$	$O_{Vacancy}$/ $O_{Lattice}$	Mo(S,O)	Co(O,S)		
MoCoOS-1	22.98	8.42	57.35	11.25	81.86	18.14	13.82	33.7	--	8.8	0.281
MoCoOS-2	18.12	12.56	55.51	13.81	81.54	18.46	22.64	33.3	11.7	8.5	0.394
MoCoOS-3	15.38	13.53	58.84	12.25	82.76	17.24	17.98	67.6	5.5	7.7	0.448
MoCoOS-4	14.75	22.76	41.69	20.80	83.43	16.57	17.05	64.1	8.7	7.4	0.585
MoCoOS-2 after reaction	16.21	10.31	53.21	14.84	82.27	17.73	21.55	34.9	12.3	--	--
Mo(S,O)	29.77	--	65.3	4.93	96.85	3.15	3.25	39.9	--	2.8	--
Co(O,S)	--	45.54	9.76	44.70	95.49	4.51	4.72	--	6.2	20.9	--

Note:* Crystal size of Mo(S,O) was calculated by (112), (-106) and (114) planes. Crystal size of Co(O,S) was calculated by (311) and (222) planes.

Table S2 XRF elemental analysis of MoCoOS

Catalyst	Elements percentage (%)			
	Mo	Co	O	S
MoCoOS-1	22.15	8.26	56.48	13.11
MoCoOS-2	17.86	12.38	55.23	14.53
MoCoOS-3	15.24	13.22	58.21	13.33
MoCoOS-4	14.68	22.65	41.52	21.15
Mo(S,O)	30.26	--	64.67	5.07
Co(O,S)	--	44.89	9.98	45.13

Table S3 EDX composition analyses and the fitting parameters of EIS analyses of Mo(S,O), Co(O,S), and MoCoOS catalysts

Catalyst	Elements percentage (%)				Electrolyte resistances (Ω)	Electron transfer resistances (Ω)	Warburg resistances (Ω)
	Mo	Co	O	S			
MoCoOS-1	21.35	8.36	57.39	12.90	0.44	2.30	1.36
MoCoOS-2	15.02	9.98	61.69	13.31	0.45	1.62	0.12
MoCoOS-3	16.38	13.59	56.25	13.78	0.44	12.57	0.56
MoCoOS-4	15.10	21.16	42.93	20.81	0.46	21.46	6.23
Mo(S,O)	27.15	--	65.32	7.53	0.52	96.30	0.90
Co(O,S)	--	42.68	15.20	42.12	0.50	584.60	--

Table S4 EDX composition analyses of Mo(S,O), Co(O,S) in MoCoOS-1

MoCoOS-1 (%)	Mo	Co	O	S
A	26.24	0.39	64.55	12.82
B	25.44	0.67	63.67	10.22
C	24.83	0.01	63.38	11.78
D	23.18	0.08	64.06	11.68
E	24.89	0.18	62.67	12.26
Mean value (A,B,C)	24.91	0.27	63.67	11.75
F	0.14	49.65	4.38	45.83
G	0.35	49.94	5.45	44.26
H	0.28	50.46	5.12	44.14
I	0.25	50.12	4.68	44.95
J	0.31	49.31	4.23	46.15
Mean value (D,E,F)	0.27	49.90	4.77	45.07

Table S5 EDX composition analyses of Mo(S,O), Co(O,S) in MoCoOS-2

MoCoOS-2 (%)	Mo	Co	O	S
A	23.12	0.28	65.95	10.65
B	23.25	0.07	66.41	10.27
C	22.83	0.33	68.46	8.38
D	22.95	0.26	68.12	9.67
E	22.55	0.29	68.21	8.95
Mean value (A,B,C)	22.94	0.25	67.43	9.58
F	0.82	48.08	6.34	44.76
G	0.41	49.71	5.35	44.53
H	0.16	51.07	6.13	42.64
I	0.65	50.25	6.20	42.9
J	0.53	49.35	4.95	45.17
Mean value (D,E,F)	0.51	49.69	5.79	44.00

Table S6 EDX composition analyses of Mo(S,O), Co(O,S) in MoCoOS-3

MoCoOS-3 (%)	Mo	Co	O	S
A	24.25	0.32	63.76	11.67
B	23.21	0.14	65.50	11.15
C	24.75	0.16	64.87	10.22
D	23.21	0.23	65.36	11.20
E	22.35	0.43	64.58	12.64
Mean value (A,B,C)	22.55	0.26	64.81	11.38
F	0.26	48.15	4.23	47.36
G	0.21	46.96	4.68	48.15
H	0.47	51.04	6.15	42.34
I	0.35	50.26	3.26	46.13
J	0.38	50.10	3.68	45.84
Mean value (D,E,F)	0.33	49.30	4.40	45.96

Table S7 EDX composition analyses of Mo(S,O), Co(O,S) in MoCoOS-4

MoCoOS-4 (%)	Mo	Co	O	S
A	21.35	1.10	64.57	12.98
B	23.47	0.73	62.54	13.26
C	24.87	0.57	62.21	12.35
D	23.36	0.68	63.76	12.20
E	22.34	0.86	65.65	11.15
Mean value (A,B,C)	23.08	0.79	63.75	12.39
F	0.58	48.12	5.32	45.98
G	0.36	46.23	5.87	47.54
H	0.35	45.49	6.02	48.14
I	0.29	46.35	3.21	50.15
J	0.45	49.34	4.28	45.93
Mean value (D,E,F)	0.41	47.11	4.94	47.55

Table S8 Comparison of the catalytic activity for various catalysts containing oxides and sulfides of cobalt and molybdenum reported in literatures for hydrogen evolution

Catalyst	Amount (mg)	Sacrifice reagent	Hydrogen rate (μmol/h)	Hydrogen rate (μmol/h/g)	λ (nm)	AQE (%)	Refs.
CoO_x/g-C_3N_4	40	10 vol.% TEOA	10.52	262.90	420	4.93	[S1]
CdS/MoS_2/Mo	10	0.35 M Na_2S, 0.25 M Na_2SO_3	12.59	1259	420	11.03	[S2]
CoO/g-C_3N_4	50	--	2.51	50.20	420	1.91	[S3]
Co(dcbpy)$_2$(NCS)$_2$/ CQDs/CN	50	10 vol.% TEOA	12.98	259.50	450	14.11	[S4]
Mo-Mo_2C/g-C_3N_4	10	20 vol.% TEOA	1.10	219.70	420	8.3	[S5]
MoS_2/g-C_3N_4	5	20 vol.% TEOA	22.48	1124	420	2.34	[S6]
$K^+CNO^-Mo_2C$	50	20 vol.% methanol	34.33	137.30	350	2.23	[S7]
Co/g-C_3N_{4-x}	100	20 vol.% methanol	75.02	750.20	450	1.92	[S8]
MoS_2/CdS-TiO_2	20	20 vol.% latic acid	280	5600	420	19.30	[S9]
Co_9S_8/$Zn_{0.5}Cd_{0.5}S$	10	0.35 M Na_2S, 0.25 M Na_2SO_3	109	10900	420	8.96	[S10]
Mo(S,O)/Co(O,S)	20	0.2 M Na_2S, 0.2 M Na_2SO_3	153.4	7670	420	14.42	This work

Table S9 Comparison of the catalytic activity of various catalysts reported in literatures for reduction 4-NP with $NaBH_4$.

Catalyst	Amount	Time (min)	Kinetic rate constant, k_{app} (min^{-1})	Ratio constant, K ($min^{-1}g^{-1}$)	Refs.
Co_3O_4	100 mg	2	0.0130	0.130	[S11]
CuO-RGO	50 mg	9	0.1500	3.000	[S12]
Pd-FG	10 mg	12	0.1410	14.100	[S13]
3D-NGF	150 mg	16	0.5256	3.504	[S14]
Ni-PVAm@SBA	120 mg	20	0.1956	1.630	[S15]
MoCoOS-2	5 mg	18	0.2112	42.244	This work

Table S10 Comparison of the catalytic activity of various catalysts reported in literatures for reduction Cr(VI) with $NaBH_4$

Catalyst	Amount	Time (min)	Kinetic rate constant, k_{app} (min^{-1})	Ratio constant, K ($min^{-1}g^{-1}$)	Refs.
Ni@Carbon	50 mg	67	0.8370	16.743	[S16]
AMD-nZVI/FeS_2	70 mg	60	0.0210	0.300	[S17]
nZVI @HCl-BC	10 mg	120	0.0033	0.330	[S18]
CuSbOS	20 mg	25	0.1930	9.650	[S19]
CuO	20 mg	70	0.0735	3.675	[S20]
MoCoOS	5 mg	18	0.2666	53.310	This work

References:

[S1] Y. Zhu, T. Wan, X. Wen, D. Chu, Y. Jiang. Tunable Type I and II heterojunction of CoO_x nanoparticles confined in g-C_3N_4 nanotubes for photocatalytic hydrogen production [J]. *Appl. Catal. B-Environ.*, 244 (2019) 814-822.

[S2] L. Zhao, J. Jia, Z. Yang, J. Yu, A. Wang, Y. Sang, W. Zhou, H. Liu. One-step synthesis of CdS nanoparticles/MoS_2 nanosheets heterostructure on porous molybdenum sheet for enhanced photocatalytic H_2 evolution [J]. *Appl. Catal. B-Environ*., 210 (2017) 290-296.

[S3] F. Guo, W. Shi, C. Zhu, H. Li, Z. Kang. CoO and g-C_3N_4 complement each other for highly efficient overall water splitting under visible light [J]. *Appl. Catal. B-Environ.*, 226 (2018) 412-420.

[S4] Y. Zhang, W. Zhang. Ternary catalysts based on amino-functionalized carbon quantum dots, graphitic carbon nitride nanosheets and cobalt complex for efficient H_2 evolution under visible light irradiation [J]. *Carbon*, 145 (2019) 488-500.

[S5] J. Dong, Y. Shi, C. Huang, Q. Wu, T. Zeng, W. Yao. A New and stable Mo-Mo_2C modified g-C_3N_4 photocatalyst for efficient visible light photocatalytic H_2 production [J]. *Appl. Catal. B-Environ*. 243 (2019) 27-35.

[S6] J. Sun, S. Yang, Z. Liang, X. Liu, P. Qiu, H. Cui, J. Tian. Two-dimensional/one-dimensional molybdenum sulfide (MoS_2) nanoflake/graphitic carbon nitride (g-C_3N_4) hollow nanotube photocatalyst for enhanced photocatalytic hydrogen production activity [J]. *J. Colloid Interf. Sci*., 567 (2020) 300-307.

[S7] D. Li, C. Zhou, X. Liang, X. Shi, Q. Song, M. Chen, D. Jiang. Noble-metal-free Mo_2C co-catalsyt modified perovskite oxide nanosheet photocatalysts with enhanced hydrogen evolution performance [J]. *Colloid. Surface. A.*, 615 (2021) article 126252.

[S8] D. Zhang, L. Peng, K. Liu, H. Garcia, C. Sun, L. Dong. Cobalt nanoparticle with tunable size supported on nitrogen-deficient graphitic carbon nitride for efficient visible light driven H_2 evolution reaction [J]. *Chem. Eng. J.*, 381 (2020) article 122576.

[S9] N. Qin, J. Xiong, R. Liang, Y. Liu, S. Zhang, Y. Li, Z. Li, L. Wu. Highly efficient photocatalytic H_2 evolution over MoS_2/CdS-TiO_2 nanofibers prepared by an electrospinning mediated photodeposition method [J]. *Appl. Catal. B-Environ.*, 202 (2017) 374-380.

[S10] X.L. Li, R.B He, Y. Dai, S. Li, N. Xiao, A. Wang, Y. Gao, N. Li, J. Gao, L. Zhang, Lei Ge. Design and fabrication of $Co_9S_8/Zn_{0.5}Cd_{0.5}S$ hollow nanocages with significantly enhanced photocatalytic hydrogen production activity [J]. *Chem. Eng. J.*, 400 (2020) 125474.

[S11] T.R. Mandlimath, B. Gopal. Catalytic activity of first row transition metal oxides in the conversion of p-nitrophenol to p-aminophenol [J]. *J. Mol. Catal. A-Chem.*, 380 (2011) 9-15.

[S12] K. Revathi, S. Palantavida, B.K. Vijayan. A Facile Method for the Synthesis of CuO-RGO Nanocomposite for Para Nitrophenol Reduction Reaction [J]. *Mater. Today-Proceeds.*, 9 (2019) 587-593.

[S13] Z. Wang, C. Xu, G. Gao, X, Lin, Facile synthesis of well-dispersed Pd–graphene nanohybrids and their catalytic properties in 4-nitrophenol reduction [J]. *Rsc. Adv.*, 4 (2014) 13644-13651.

[S14] J. Liu, X. Yan, L. Wang, L. Kong, P. Jian. Three-dimensional nitrogen-doped graphene foam as metal-free catalyst for the hydrogenation reduction of p-nitrophenol [J]. *J. Colloid. Interf. Sci.*, 497 (2017) 102-107.

[S15] R.J. Kalbasi, A.A. Nourbakhsh, F. Babaknezhad. Synthesis and characterization of Ni nanoparticles-polyvinylamine/SBA-15 catalyst for simple reduction of aromatic nitro compounds [J]. *J. Catal. Commun.*, 12 (2011) 955-960.

[S16] Z. Lv, X. Tan, C. Wang, A. Alsaedi, T. Hayat, C. Chen. Metal-organic frameworks-derived 3D

yolk shell-like structure Ni@carbon as a recyclable catalyst for Cr(VI) reduction [J]. *Chem. Eng. J.*, 389 (2020) article 123428.

[S17] Z.H. Diao, L. Yan, F.X. Dong, Z-L. Chen, P.R. Guo, W. Qian, W.X. Zhang, J.Y. Liang, S.T. Huang, W. Chu. Ultrasound-assisted catalytic reduction of Cr(VI) by an acid mine drainage based *n*ZVI coupling with FeS_2 system from aqueous solutions: Performance and mechanism [J]. *J. Environ. Manage*., 278 (2021) article 111518.

[S18] H. Dong, J. Deng, Y. Xie, C. Zhang, Z. Jiang, Y. Cheng, K. Hou, G. Zeng. Stabilization of nanoscale zero-valent iron (*n*ZVI) with modified biochar for Cr(VI) removal from aqueous solution [J]. *J. Hazard. Mater*., 332 (2017) 79-86.

[S19] X.Y. Chen, D.H. Kuo, J.B. Zhang, Qi.X. Lu, J.G. Lin. Nanosheet bimetal oxysulfide CuSbOS catalyst for highly efficient catalytic reduction of heavy metal ions and organic dyes [J]. *J. Mol. Liq*., 275 (2019) 204-214.

[S20] Z.H. Xu, Y.Q. Yu, D. Fang, J.R. Liang, L.X. Zhou. Simulated solarlight catalytic reduction of Cr(VI) on microwave–ultrasonication synthesized flower-like CuO in the presence of tartaric acid [J]. *Mater. Chem. Phys*., 171 (2016) 386-393.